Anal. Chem. **2002,** *74,* 6244−6251

Retention of Carbon and Alteration of Expected ^{13}C-Tracer Enrichments by Silylated Derivatives Using Continuous-Flow Combustion-Isotope Ratio Mass Spectrometry

Steven R. Shinebarger, Michael Haisch, and Dwight E. Matthews*

Departments of Medicine and Chemistry, The University of Vermont, Burlington, Vermont 05405

Continuous-flow inlets from oxidation reactors are commonly used systems for biological sample introduction into isotope ratio mass spectrometers (IRMS) to measure ^{13}C enrichment above natural abundance. Because the samples must be volatile enough to pass through a gas chromatograph, silylated derivatization reactions are commonly used to modify biological molecules to add the necessary volatility. Addition of a *tert*-butyldimethylsilyl (TBDMS) group is a common derivatization approach. However, we have found that samples do not produce the expected increment in measured ^{13}C abundance as the TBDMS derivatives. We have made measurements of ^{13}C enrichment of leucine and glutamate standards of known ^{13}C enrichment using derivatives without silicon (*N*-acetyl *n*-propyl ester), with silicon (TBDMS), and an intermediate case. The measurements of ^{13}C in amino acids derivatized without silicon were as expected. The ^{13}C enrichment measurements using the TBDMS derivative were higher than expected but could be corrected to produce the expected ^{13}C enrichment measurement by IRMS if one carbon was removed per silicon. We postulate that the silicon in the derivative forms silicon carbide compounds in the heated cupric oxide reactor, rather than forming silicon dioxide. Doing so reduces the amount of CO_2 formed from the carbon in the sample. Silylated derivatives retain carbon with the silicon and must be used carefully and with correction factors to measure ^{13}C enrichments by continuous-flow IRMS.

Isotope ratio mass spectrometry (IRMS) has been used since the 1940s to determine ^{13}C abundance at natural levels. The technology did not change significantly until resurgence for measurement of ^{13}C tracer molecules in biological samples in the 1980s using continuous-flow systems.[1−5] The key advantage of IRMS has always been its sensitivity to measure very fine differences in ^{13}C abundance, but its key limitation is that IRMS only measures ^{13}C in CO_2. All compounds to be measured must be isolated, purified, and oxidized to CO_2 prior to measurement by IRMS. Because biological compounds usually exist in complex matrixes (e.g., blood), isolation of a specific compound in sufficient quantities for IRMS measurement is difficult. However, the introduction of gas chromatography-combustion-IRMS (GC/C-IRMS) resolved these problems.[6] The GC/C-IRMS puts a GC in front to provide separation of mixtures of compounds, prior to their oxidation in the flow-through combustion tube and entrance into the IRMS.[4,5,7] The introduction of samples by a continuous flow of helium carrier gas allows delivery of very small amounts of sample into the IRMS and greatly improves the sensitivity of the IRMS to measure $^{13}CO_2$ from metabolites in biological matrixes.[4] Although procedures have been devised to chemically modify biological compounds with out adding carbon,[8] most biological compounds must be chemically modified ("derivatized") to make them volatile enough to pass through the GC prior to measurement.[9] A popular derivatization approach is to form the *tert*-butyl dimethyl silyl (TBDMS) derivative. Because the TBDMS group can be attached to almost all functional groups, it is a good choice for derivatizing polyfunctional species, such as amino acids.[10,11]

The derivatization process, however, adds C to the molecule, and this C becomes part of the total C measured when the compound is oxidized to CO_2. The ^{13}C abundance of the core molecule can be determined if the ^{13}C abundance of the derivative is known. In many cases, it is not. However, most biological applications using GC/C-IRMS make measurements of ^{13}C-labeled compounds are administered to animals or humans as tracers for the purpose of determining in vivo kinetics. For ^{13}C tracer applications, it is simple enough to prepare a standard curve of known *^{13}C tracer content* (either mole fraction of ^{13}C tracer against unlabeled or mole ratio of ^{13}C tracer against unlabeled) by mixing known amounts of the ^{13}C-labeled compound with known amounts

* Corresponding author. E-mail: Dwight.Matthews@uvm.edu. Voice: (802) 656-8114. Fax: (802) 656-8705.

(1) Klein, P. D. *Fed. Proc.* **1982**, *41*, 2698−701.
(2) Bier, D. M.; Matthews, D. E. *Fed. Proc.* **1982**, *41*, 2679−85.
(3) Matthews, D. E.; Bier, D. M. *Annu. Rev. Nutr.* **1983**, *3*, 309−39.
(4) Brand, W. A. *J. Mass Spectrom.* **1996**, *31*, 225−35.
(5) Brenna, J. T.; Corso, T. N.; Tobias, H. J.; Caimi, R. J. *Mass Spectrom. Rev.* **1997**, *16*, 227−58.
(6) Matthews, D. E.; Hayes, J. M. *Anal. Chem.* **1978**, *50*, 1465−73.
(7) Brenna, J. T. *Rapid Commun. Mass Spectrom.* **2001**, *15*, 1252−62.
(8) Zaideh, B. I.; Saad, N. M.; Lewis, B. A.; Brenna, J. T. *Anal. Chem.* **2001**, *73*, 799−802.
(9) Knapp, D. R. *Handbook of Analytical Derivatization Reactions*; John Wiley: New York, 1979.
(10) Mawhinney, T. P.; Robinett, R. S. R.; Atalay, A.; Madson, M. A. *J. Chromatogr.* **1986**, *358*, 231−42.
(11) Chaves Das Neves, H. J.; Vasconcelos, A. M. P. *J. Chromatogr.* **1987**, *392*, 249−58.

10.1021/ac026061s CCC: $22.00
Published on Web 11/16/2002

of unlabeled compound. These standard samples are derivatized and measured by GC/C-IRMS.

Because the C added by the derivative adds to the total CO_2 produced when the derivatized compound is oxidized, the measured $^{13}C/^{12}C$ ratio of the tracer will be reduced by the amount of C added by the derivatization process. This effect is seen by plotting the measured ^{13}C mole fraction from the GC/C-IRMS against the ^{13}C mole fraction of the tracer dilution standards. A 1:1 response (slope of unity) of the IRMS system is expected for $^{13}C/^{12}C$ measurement. However, the slope of the line of the IRMS-measured ^{13}C enrichment from the CO_2 versus the prepared ^{13}C-labeled-to-unlabeled ratio of the standards will be less than unity by the amount of C added from the derivative. This dilution can be corrected because we know the total number of unlabeled and labeled carbons in the molecule. A simple mass balance equation can be used to convert from the ^{13}C content of the total molecule to the ^{13}C content for the specific carbons in the molecule that are labeled. Doing so will change the measured slope upward to equal unity.

Because a CO_2 gas of known ^{13}C content is pulsed into the ion source during a GC/C-IRMS run to define and normalize the $^{13}C/^{12}C$ ratio measurement, many investigators do not prepare and run standard curves of their ^{13}C-labeled tracers. They assume that the response of the IRMS will be 1:1 in terms of the measured $^{13}C/^{12}C$ ratio for the amount of ^{13}C put in. This assumption is correct, with certain exceptions that have nothing to do with the IRMS system. Our practice is to compare our GC/C-IRMS measurements against standards of known ^{13}C content of every new tracer and derivative we use. Normally we obtain the expected 1:1 ^{13}C response from the GC/C-IRMS, after adjusting for the amount of C added to the compound by the derivatization. However, when we began measuring TBDMS derivatives of ^{13}C-labeled amino acids, we observed slopes significantly greater than unity *after* correcting for total C. We believe these higher-than-unity slopes occur because silicon in the TBDMS sequesters C in the combustion tube during the oxidation process; i.e., the silicon does not oxidize completely in the combustion tube to SiO_2, but forms silicon carbide complexes. Silicon carbide formation reduces the amount of total CO_2 formed from the sample and alters the conversion calculations of measured ^{13}C tracer enrichment. This paper presents the data to confirm this hypothesis.

EXPERIMENTAL SECTION

Instrumentation and Conditions. A Finnigan Delta Plus (Finnigan MAT, Bremen, Germany) GC/C-IRMS with a GCC-III interface and a HP6890 gas chromatograph (Agilent, Palo Alto, CA) was exclusively used. Samples were injected by a CTC-A200S autosampler (CTC Analytics, Zwingen, Switzerland) mounted to the HP6890 GC. The effluent from the GC passed immediately into and through a standard Finnigan alumina oxidation tube (0.5-mm i.d. × 1.55-mm o.d. × 320 mm) containing cupric oxide wires, 240 mm in length. The oxidation tube was held at 960 °C. The effluent then passed through a water separator consisting of a Nafion tube in the GCC-III interface prior to entering the mass spectrometer.

The GC column used for all measurements was a 30-m × 250-μm-i.d., 0.250-μm film thickness Zebron ZB-5 (Phenomenex, Torrance, CA) fused-silica capillary column. For measuring leucine samples, a 20:1 split of sample in the inlet, a helium column flow of 2.2 mL/min, and an inlet temperature of 265 °C were used. The GC temperature program was an initial temperature of 160 °C, increased to 190 °C at 2 °C/min. For glutamate samples, a 35:1 inlet split at 265 °C and a helium flow of 2.2 mL/min were used. The GC program was 162 °C isothermal for 11 min followed by ramping the temperature to 200 °C for 5 min. For all samples, 1 μL was injected into the GC. The effluent from the GC was diverted away from the oxidation tube during the initial period of solvent elution and out a divert valve to the atmosphere while helium was passed backward through the oxidation tube. After the solvent had completely eluted from the column, the divert valve was automatically closed, and the GC effluent returned to passing through the oxidation tube. During the solvent-divert period, CO_2 gas of known ^{13}C content was automatically cycled into the IRMS and its $^{13}C/^{12}C$ ratio measured. After the solvent-divert period, the effluent from the GC and oxidation tube entered the IRMS. The IRMS automatically measured the ion intensities of $m/z = 44$, 45, and 46 in its three Faraday cups, corresponding to $^{12}C^{16}O_2$, $^{13}C^{16}O_2 + {}^{12}C^{16}O^{17}O$, and $^{12}C^{16}O^{18}O$, respectively. The Finnigan Isodat data system automatically computed the $^{13}C/^{12}C$ with an ^{17}O correction and $^{18}O/^{16}O$ ratios of each sample peak, referenced to the standard CO_2 gas and its known $^{13}C/^{12}C$ and $^{18}O/^{16}O$ content. These data were then used here for the various samples measured.

Reagents and Chemicals. Triethylamine, 1-propanol, acetic anhydride, ethyl acetate, acetyl chloride, and acetone at >99% purity were obtained from Sigma-Aldrich (St. Louis, MO). Acetonitrile at 99.99% purity was purchased from EM Science (Gibbstown, NJ). *N*-Methyl-*N*-(*tert*-butyldimethylsilyl)trifluoroacetamide (MTBSTFA) was purchased from Regis Technologies (Morton Grove, IL).

L-[1,2-$^{13}C_2$]Leucine was purchased from Mass Trace (Woburn, MA), and L-[1,2-$^{13}C_2$]glutamic acid was purchased from Cambridge Isotope Laboratories (Andover, MA). The [1,2-$^{13}C_2$]leucine was measured by gas chromatography/mass spectrometry (GC/MS) to have a chemical purity of 100% and a ^{13}C isotopic content of 98.4% in carbon positions 1 and 2. The [1,2-$^{13}C_2$]glutamic acid was measured by GC/MS to have a chemical purity of 95.3% and a ^{13}C isotopic content of 97.5% in carbon positions 1 and 2. Unlabeled L-leucine and L-glutamate were purchased from Sigma-Aldrich with an assumed chemical purity of >99%.

Quantitative solutions of [1,2-$^{13}C_2$]leucine and [1,2-$^{13}C_2$]glutamate were prepared by weighing tared containers before and after addition of aliquots of the labeled amino acids and distilled water. Three standards of known ^{13}C content in the range of 0−0.6 mol % excess (mpe) [1,2-$^{13}C_2$]leucine and [1,2-$^{13}C_2$]glutamate were prepared in a two-step process. First, containers were weighed before and after adding amounts of the [1,2-$^{13}C_2$]leucine or [1,2-$^{13}C_2$]glutamate standard solutions. Next, amounts of unlabeled leucine or glutamate were added to the containers, and the containers were weighed again. Unlabeled standards were made by adding no labeled material. Distilled water was then added to the containers to dilute the leucine or glutamate to concentrations of ~30 mM. About ~1-μmol aliquots of these various solutions were taken for derivatization and measurement.

Reagent solutions were first prepared for the formation of the *N*-acetyl *n*-propyl ester (NAP) derivatives described below. Propylating reagent was formed by mixing acetyl chloride with ice-

Table 1. Carbon Content of the Different Leucine and Glutamate Derivatives Tested[a]

amino acid core	derivative type	derivative species added to the		number of carbons			no. of silicons
		amino N	carboxyl group	core	derivative	total	
leucine	NAP	CH_3CO	C_3H_7	6	5	11	0
	TBDMS	$Si(CH_3)_2C_4H_9$	$Si(CH_3)_2C_4H_9$	6	12	18	2
	mixed	$Si(CH_3)_2C_4H_9$	C_3H_7	6	9	15	1
glutamate	NAP	CH_3CO	C_3H_7	5	8	13	0
	TBDMS	$Si(CH_3)_2C_4H_9$	$Si(CH_3)_2C_4H_9$	5	18	23	3
	mixed	$Si(CH_3)_2C_4H_9$	C_3H_7	5	12	17	1

[a] NAP, *N*-acetyl *n*-propyl ester; TBDMS, *tert*-butyldimethylsilyl ester; and mixed, *N*-acetyl *tert*-butyldimethylsilyl ester.

cold propanol at a ratio of 6.25:1 with constant stirring. Acetylating agent was prepared by mixing acetone, triethylamine, and acetic anhydride in the ratio of 5:2:1 with constant stirring.

Derivatization of Amino Acids. Leucine and glutamate samples were derivatized in 2-mL conical-bottom glass screw-cap vials as the NAP and TBDMS esters. In addition, a third derivative type was made that was mixture of the NAP and TBDMS (designated "mixed"). For preparation of the NAP derivatives, aqueous aliquots of the amino acids were taken and dried under nitrogen gas in the 2-mL vials. Propylating reagent (350 μL) was added to each vial, and the vials were capped and heated at 75 °C for 35 min. The reagents were evaporated from the vials by drying under a stream of nitrogen gas. Next, 500 μL of acetylating reagent was added, and the vials were capped and heated at 75 °C for 35 min. The reagent was then removed by evaporation under a stream of nitrogen. Sufficient ethyl acetate was added to the vials as the final solvent to give an amino acid concentration of 9 nmol/μL.

TBDMS derivatives were prepared by first drying aqueous aliquots of the amino acids under nitrogen gas. A 50-μL 1:1 mixture of MtBSTFA/acetonitrile was added to each of the vials, and the vials were capped and heated at 100 °C for 40 min. Additional acetonitrile was added to obtain a final amino acid concentration of 9 nmol/μL.

The "mixed" derivatives were formed by first drying aqueous aliquots of the amino acids under a nitrogen gas in the vials and propylated as described above. After the propylating mixture had been evaporated under a stream of nitrogen gas, a 50-μL mixture of the 1:1 MtBSTFA/acetonitrile was then added to each of the vials, and the vials were capped and heated at 100 °C for 30 min. Acetonitrile was added to obtain a final amino acid concentration of 9 nmol/μL.

Rationale for Derivative and Amino Acid Choices. The NAP derivative was chosen because it adds no silicon and could be used to compare the effects of adding silicon by the TBDMS derivative. As shown in Table 1, the NAP derivative adds an acetyl group to the amino N and a propyl group to the carboxyl. The TBDMS derivative adds a TBDMS group to both amino N and carboxylic acid functional groups. The mixed derivative was chosen to form an intermediate case: one TBDMS group added to the amino N and a propyl group to the carboxylic acids (Table 1). Leucine was chosen as one test amino acid because it has a single carboxylic acid and amino group without any additional functional groups (Figure 1). Glutamate was chosen because it has *two* carboxylic acids and a single amino group (Figure 1). The number of silyl groups range from 0 to 3 for the two amino acids and three derivative types (Table 1). The key differences between glutamate and leucine are both the number of silyl derivatives added and the location. These differences provide enough different cases for study to define whether an effect of silicone is specific to amino N-bonded silyl, O-bonded silyl, or equally similar for both types.

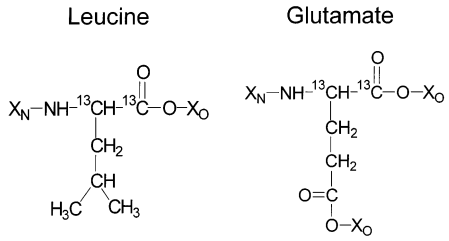

Figure 1. Chemical structures of leucine and glutamic acid with the location of the derivative shown. The derivative located on the amino N is marked with an X_N and derivative on the carboxyl group is marked with an X_O. The structures of X_N and X_O vary with the derivative type and are shown in Table 1. Note that glutamate contains two carboxylic groups and will have two X_O units attached for each derivative used.

Experiments. Derivatives were prepared for each of the [1,2-$^{13}C_2$]leucine and [1,2-$^{13}C_2$]glutamate enrichment standard solutions for each derivative type: NAP, TBDMS, and mixed. Each of these derivatives was then injected into the GC/C-IRMS in replicate. Pulses of CO_2 reference gas of known ^{13}C content were also admitted several times during each GC/C-IRMS run. The peaks for both the reference gas and the samples were automatically integrated by the data system on each run and the ^{13}C content of each sample peak determined in units relative to the reference gas measurements:

$$\delta^{13}C_{(ref)} = (R_{sample}/R_{ref} - 1) \times 1000 \quad (1)$$

where R_{sample} and R_{ref} are the GC/C-IRMS-measured $^{13}C/^{12}C$ ratios of the sample and reference gas CO_2 peaks, respectively. The $\delta^{13}C_{(ref)}$ was corrected for ^{17}O contributions. Because the reference tank gas had been standardized to PDB, the $\delta^{13}C_{(ref)}$ was converted to a delta value referenced to PDB ($\delta^{13}C_{PDB}$). All of these calculations were performed automatically by the Finnigan Isodat data system.

The $^{13}C/^{12}C$ ratio of the sample was then calculated from its measured delta value by rearranging eq 1:

$$(^{13}C/^{12}C)_{sample} = [\delta^{13}C_{PDB}/1000 + 1](^{13}C/^{12}C)_{PDB} \quad (2)$$

where $(^{13}C/^{12}C)_{PDB}$ was assumed to be 0.011 237 2. The $(^{13}C/^{12}C)_{sample}$ ratio values for each measurement were then used in the calculations outlined below.

Enrichment Calculations. The $^{13}C/^{12}C$-measured ratio of each sample was converted to ^{13}C abundance (F):

$$F = (^{13}C/^{12}C)/[1 + (^{13}C/^{12}C)] \quad (3)$$

This ^{13}C abundance is the abundance of ^{13}C in the entire molecule and is usually expressed as atom percent ^{13}C. This abundance can be separated into the portion that is labeled with ^{13}C and that which is not by simple mass balance:

$$NF = (N - n_l)F_u + n_lF_l \quad (4)$$

where N is the total number of carbons in the derivatized molecule, n_l is the number of carbons that are labeled with ^{13}C in the molecule, F_u is the ^{13}C abundance of the unlabeled carbons, and F_l is the ^{13}C abundance of the carbon in the positions containing the labels (always positions 1 and 2 in the amino acid samples used in this study).

This equation can be simplified by considering only the ^{13}C in *excess of natural abundance* in the sample, i.e., subtracting the natural abundance contribution (NF_u) from both sides. Doing so reduces eq 4 to

$$N(F - F_u) = n_l(F_l - F_u) \quad (5)$$

This subtraction is normally done by measuring an unlabeled sample (sample 0) of natural ^{13}C abundance (F_0) and subtracting this ^{13}C abundance from all other samples. This subtraction gives the ^{13}C enrichment in excess above natural abundance: $E = F - F_0$, usually expressed as atom percent excess ^{13}C (ape). Substituting, F_0 for F_u in eq 5, gives

$$NE = n_lE_l \quad (6)$$

where E is the enrichment in excess of natural abundance in the whole molecule and E_l is the enrichment in excess of natural abundance of the labeled C in the molecule. This equation can be rearranged to determine the average ^{13}C enrichment in the labeled portion of the molecule in excess of natural abundance ($E_l = F_l - F_0$) relative the measured ^{13}C enrichment of the whole molecule:

$$E_l = EN/n_l \quad (7)$$

The ^{13}C enrichment in the labeled positions of each standard (F_l) was defined from the amounts of unlabeled and labeled amino acids mixed together for each standard using the following mass balance dilution equation:

$$F_l = (x_{(l)}\,F_{l(l)} + x_{(u)}F_0)/(x_{(l)} + x_{(u)}) \quad (8)$$

where $x_{(l)}$ and $x_{(u)}$ are the amounts of labeled amino acid and unlabeled amino acid, respectively, in the solution in moles and $F_{l(l)}$ is the GC/MS-determined average ^{13}C enrichment in atom percent in the labeled positions of the labeled amino acid. Note that F_l is the enrichment in atom percent of the ^{13}C in the labeled positions in the molecule, be it leucine or glutamate standards. The enrichment of ^{13}C in the whole molecule is lower due to the presence of unlabeled C from the other carbons in the amino acid that are not labeled and the addition of C from the derivatives. The enrichment of ^{13}C in the whole molecule (F) can be calculated from F_l according to eq 4 above. The ^{13}C enrichment above natural abundance (atom % excess) in the labeled positions of these standards is simply $E_l = F_l - F_0$, where F_0 is the natural abundance ^{13}C value defined above.

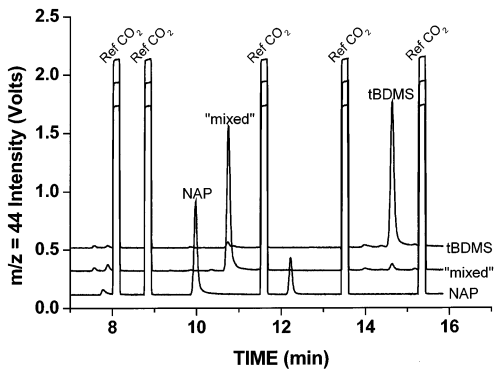

Figure 2. Time course of leucine measured by GC/C-IRMS. The graph plots the intensity versus time of the $m/z = 44$ CO_2^+ ion signal. The graph is a composite of three injections: one for each derivative type. The three injections are deliberately offset from each other on the *y*-axis to make the three traces distinguishable. The "square wave" peaks are injection of the reference tank CO_2 gas into the system (denoted "Ref CO_2") and occur before and after elution of each of the leucine derivatives. Elution order of the leucine derivatives was *N*-acetyl *n*-propyl ester (NAP), *tert*-butyldimethylsilyl *n*-propyl ester ("mixed"), and bis(*tert*-butyldimethylsilyl) ester (TBDMS).

Statistics. Linear least-squares regression analyses were performed on each standard curve measured. Standard errors of both the intercept and slope were calculated in the process. From these data, the slope of each regression line was tested by a two-tailed *t*-test for being different from unity.[12] A P value of <0.05 defined significance. All data are expressed as mean ± standard error or ± standard deviation, as indicated.

RESULTS

Simple GC programs were used to measure all three derivatives for leucine and for glutamate. Figure 2 shows the GC/C-IRMS time course of each of the three different leucine derivatives eluting from the column and being measured by the GC/C-IRMS system. The figure is a composite of three injections: one for each derivative type. Each trace is offset from the other on the *y*-axis to make them distinguishable. The peaks that appear as "square waves" in each of the traces represent the automatic injection of the CO_2 reference gas. Although the $m/z = 44$, 45, and 46 signal intensities are simultaneously recorded by separate Faraday cups, only the $m/z = 44$ signal intensity is shown in Figure 2. The elution order of the different leucine derivatives was NAP, mixed, and TBDMS.

Figure 3 shows the time course of the three different glutamate derivatives eluting and being measured ($m/z = 44$) by the GC/

(12) Zar, J. H. *Biostatistical Analysis*; Prentice Hall: Englewood Cliffs, NJ, 1974.

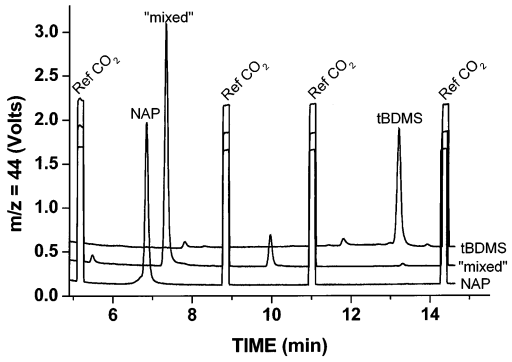

Figure 3. Time course of glutamate measured by GC/C-IRMS. The graph plots the intensity versus time of the $m/z = 44$ CO_2^+ ion signal under the same conditions as described in Figure 2.

Table 2. GC/C-IRMS Leucine Data for the Three Derivatives Tested[a]

		expected ^{13}C enrichment		measured ^{13}C enrichment			
sample ID	derivative type	E (ape)	E_l (ape)	$\delta^{13}C_{PDB}$ (per mil)	F (atom %)	E (ape)	E_l (ape)
natural	NAP	0.0000	0.0000	−31.95 ±0.45	1.0761 ±0.0005	0.0000	0.0000
std 1	NAP	0.0350	0.1928	1.04 ±0.21	1.1124 ±0.0002	0.0363	0.1994
std 2	NAP	0.0663	0.3647	27.95 ±0.48	1.1419 ±0.0005	0.0658	0.3620
natural	mixed	0.0000	0.0000	−28.12 ±0.23	1.0803 ±0.0003	0.0000	0.0000
std 1	mixed	0.0257	0.1928	−2.48 ±0.50	1.10851 ±0.0006	0.0257	0.2115
std 2	mixed	0.0486	0.3647	19.93 ±0.29	1.1331 ±0.0003	0.0486	0.3961
natural	tBDMS	0.0000	0.0000	−27.77 ±0.19	1.0809 ±0.0002	0.0000	0.0000
std 1	tBDMS	0.0214	0.1928	−5.81 ±0.10	1.1049 ±0.0001	0.0214	0.2172
std 2	tBDMS	0.0405	0.3647	14.14 ±0.31	1.1268 ±0.0003	0.0405	0.4145

[a] E, ^{13}C enrichment in the entire derivatized molecule; E_l, ^{13}C enrichment in the two labeled carbons (C-1 and C-2) in the leucine; F, the measured ^{13}C in the derivatized molecule; NAP, *N*-acetyl *n*-propyl ester; TBDMS, *tert*-butyldimethylsilyl ester; and mixed, *N*-acetyl *tert*-butyldimethylsilyl ester.

C-IRMS system. Different GC programs and placement of reference CO_2 peaks were used for glutamate compared to leucine. The elution order of the glutamate derivatives was NAP, mixed, and then TBDMS.

The measurements of the [1,2-$^{13}C_2$]leucine standards for each derivative type are shown in Table 2. The three samples are an unlabeled leucine sample and two unlabeled leucine samples to which small amounts of [1,2-$^{13}C_2$]leucine have been added (std 1 and std 2). The enrichments of the standards are defined relative to the unlabeled leucine and are 0.193 and 0.365 atom % excess for std 1 and std 2, respectively. These enrichments are the average ^{13}C enrichment in the 1- and 2-C in the [1,2-$^{13}C_2$]leucine (E_l) and are the same among the different derivatives. When these standards are oxidized to CO_2, their enrichments (E) are less than the enrichment in the labeled positions due to dilution of C both in the leucine and that C added by the derivative. The expected ^{13}C enrichments are shown for each standard and derivative type in Table 2. The E values vary by derivative for two enriched standards.

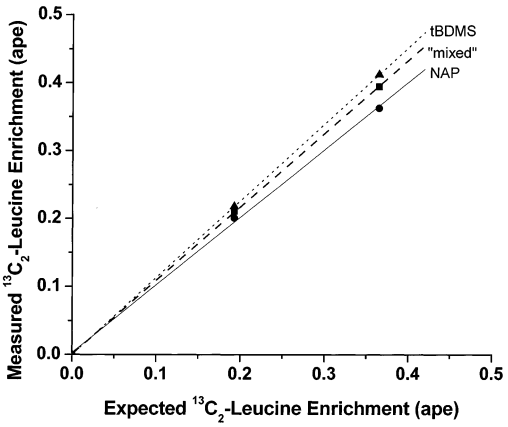

Figure 4. Measured ^{13}C enrichment versus expected ^{13}C enrichment for the [1,2-$^{13}C_2$]leucine enrichment standards. The data for the three standards (natural, std 1, and std 2) plotted in this figure are presented in Table 2 for the E_l columns, i.e., the average enrichment in the ^{13}C of positions 1 and 2 in the labeled molecule. The regression lines for the three derivatives are $E_{l(msrd)} = (0.003 \pm 0.003) + (0.994 \pm 0.011)E_{l(std)}$ for the NAP derivative ($r^2 = 0.9992$); $E_{l(msrd)} = (0.001 \pm 0.002) + (1.087 \pm 0.007)E_{l(std)}$ for the mixed derivative ($r^2 = 0.9997$), and $E_{l(msrd)} = (0.000 \pm 0.001) + (1.136 \pm 0.005)E_{l(std)}$ for the TBDMS derivative ($r^2 = 0.9999$). The slope of each line was tested for a difference from a value of unity by a two-tailed *t*-test. The slope of the NAP-leucine line was not statistically different from unity, but both the mixed and tBDMS derivatives slopes were significantly different ($p < 0.001$ for both).

The GC/C-IRMS data system automatically calculates the ^{13}C content of each sample as $\delta^{13}C$ versus PDB. These values are shown in Table 2 as measured; they were converted first to mole fraction of ^{13}C (F), then to enrichment of ^{13}C in the whole molecule (E), and finally to ^{13}C enrichment in the labeled positions. This latter measured term (E_l) is independent of the amount of C added by the derivative and makes it possible to compare measurements among derivatives. The measured E_l enrichments in Table 2 are plotted in Figure 4 against the expected E_l enrichment values for each standard and derivative type. The anticipated result is that a 1-unit increase in ^{13}C enrichment will produce a 1-unit increase in *measured* ^{13}C enrichment. The slope of the measured versus expected ^{13}C enrichment for the NAP-leucine derivative was as predicted: not distinguishable from unity (Figure 4). However, the slopes for both the mixed derivative and the TBDMS derivative were significantly greater than unity and significantly greater than the NAP-leucine slope.

The measurements of the [1,2-$^{13}C_2$]glutamate standards as each derivative type are shown in Table 3. The three samples are an unlabeled and two unlabeled glutamate samples, similar to those used for leucine. The enrichments are defined for glutamate, as they were for leucine: the average ^{13}C enrichment in the 1- and 2-C in the [1,2-$^{13}C_2$]glutamate (E_l). When these standards are oxidized to CO_2 as their derivatized molecules, the enrichments of the resulting CO_2 (E) are less than the enrichments in the labeled positions due to dilution of C from the glutamate and that added the derivative. The expected ^{13}C enrichments are shown for each standard and derivative type in Table 3. The E values vary by derivative for two enriched standards.

The measured $\delta^{13}C$ values for the glutamate standards (Table 3) were converted to mole fraction of ^{13}C (F), then to enrichment of ^{13}C in the whole molecule (E), and finally to ^{13}C enrichment in

Table 3. GC/C-IRMS Glutamate Data for the Three Derivatives Tested[a]

		expected ^{13}C enrichment		measured ^{13}C enrichment			
sample	derivative type	E (ape)	E_l (ape)	$\delta^{13}C_{PDB}$ (per mil)	F (at. %)	E (ape)	E_l (ape)
natural	NAP	0.0000	0.0000	−33.54 ±0.52	1.0744 ±0.0006	0.0000	0.0000
std 1	NAP	0.0364	0.2368	−1.31 ±0.09	1.1098 ±0.0001	0.0354	0.2303
std 2	NAP	0.0800	0.5202	−40.45 ±0.19	1.1557 ±0.0002	0.0813	0.5284
natural	mixed	0.0000	0.0000	−30.43 ±0.09	1.0778 ±0.0001	0.0000	0.0000
std 1	mixed	0.0279	0.2368	−2.92 ±0.17	1.1080 ±0.0002	0.0302	0.2570
std 2	mixed	0.0612	0.5202	29.10 ±0.19	1.1432 ±0.0002	0.0654	0.5560
natural	tBDMS	0.0000	0.0000	−28.29 ±0.22	1.0801 ±0.0002	0.0000	0.0000
std 1	tBDMS	0.0197	0.2368	−7.93 ±0.06	1.1025 ±0.0001	0.0224	0.2685
std 2	tBDMS	0.0433	0.5201	16.19 ±0.38	1.1290 ±0.0004	0.0489	0.5866

[a] E, ^{13}C enrichment in the entire derivatized molecule; E_l, ^{13}C enrichment in the two labeled carbons (C-1 and C-2) in the glutamate; F, the measured ^{13}C in the derivatized molecule; NAP, *N*-acetyl *n*-propyl ester; TBDMS, *tert*-butyldimethylsilyl ester; and mixed, *N*-acetyl *tert*-butyldimethylsilyl ester.

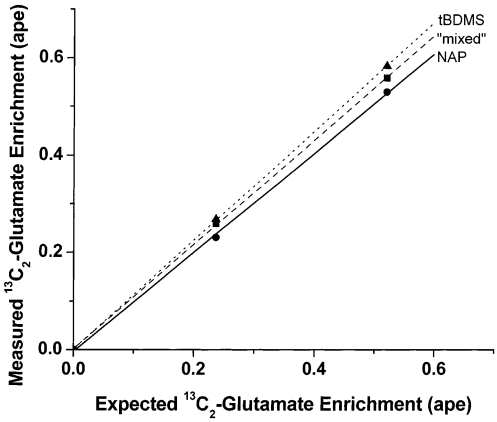

Figure 5. Measured ^{13}C enrichment versus expected ^{13}C enrichment for the [1,2-$^{13}C_2$]glutamate enrichment standards. The data for the three standards (natural, std 1, and std 2) plotted in this figure are presented in Table 3 for the E_l columns, i.e., the average enrichment in the ^{13}C of positions 1 and 2 in the labeled molecule. The regression lines for the three derivatives are $E_{l(msrd)} = (-0.004 \pm 0.003) + (1.017 \pm 0.009)E_{l(std)}$ for the NAP derivative ($r^2 = 0.9995$); $E_{l(msrd)} = (0.001 \pm 0.001) + (1.069 \pm 0.004)E_{l(std)}$ for the mixed derivative ($r^2 = 0.9999$), and $E_{l(msrd)} = (0.001 \pm 0.002) + (1.128 \pm 0.005)E_{l(std)}$ for the TBDMS derivative ($r^2 = 0.9999$). The slope of each line was tested for a difference from a value of unity by a two-tailed *t*-test. The slope of the NAP-glutamate line was not statistically different from unity, but both the mixed and tBDMS derivatives slopes were significantly different ($p < 0.001$ for both).

the labeled positions (E_l). The measured E_l enrichments in Table 3 are plotted in Figure 5 against the expected E_l enrichment values for each standard and derivative type. The anticipated result was that each derivative type would produce a slope of unity. The slope of the measured versus expected ^{13}C enrichment for the NAP-glutamate derivative was not distinguishable from unity (Figure 5). However, the slopes for both the mixed derivative and the TBDMS derivative were significantly greater than unity and significantly greater than the NAP-glutamate slope.

DISCUSSION

Because the same ^{13}C amino acid standards produced different measured ^{13}C enrichments by GC/C-IRMS as different derivatives, we conclude that the derivative type affects the result. The difference among the three derivative types and two amino acids tested is the amount of silicon present. The samples without silicon (NAP derivative) produced the anticipated GC/C-IRMS response of an equal increase in measured ^{13}C signal for an increase of ^{13}C in the sample. However, both the TBDMS derivative and the mixed derivative produced ^{13}C measurements greater than expected (Figures 4 and 5). We believe that the silicon does not proceed to SiO_2 in the oxidation tube but forms a silicon carbide (SiC_x) compound. Any carbon retained as silicon carbide in the oxidation tube would be unavailable to form CO_2 and would not dilute the ^{13}C in the labeled ^{13}C standards as expected.

A term for the amount of carbon retained by silicon that does not appear as CO_2 when the sample is oxidized, X, can be included into eq 4:

$$(N - X)F = (N - X - n_l)F_u + n_l F_l \qquad (9)$$

where N is the total number of carbon atoms in the derivatized molecule, n_l is the number of carbon atoms that are labeled with ^{13}C in the molecule, X is the number of C atoms retained by Si, F_u is the ^{13}C abundance of unlabeled carbon in the molecule, and F_l is the ^{13}C abundance of the carbon in the positions containing the labels (always positions 1 and 2 in the amino acid samples used in this study). This equation can be simplified by first rearranging eq 9

$$(N - X)F = (N - X)F_u + n_l(F_l - F_u) \qquad (10)$$

and then subtracting $(N - X)F_u$ from each side

$$(N - X)(F - F_u) = n_l(F_l - F_u) \qquad (11)$$

converting from terms using mole fraction (F terms) to enrichment above natural abundance (E terms where $E = F - F_u$). The term F_u cannot be evaluated directly, but we can substitute the measurement of ^{13}C abundance for the unlabeled standard in for F_u: $E = F - F_0$. Doing so, reduces eq 11 to

$$(N - X)E = n_l E_l \qquad (12)$$

where E is the ^{13}C enrichment (atom % excess) in the whole molecule (measured as CO_2) and E_l is the ^{13}C enrichment (atom % excess) in the labeled positions. This equation can be rearranged

$$E_l = E\,(N - X)/n_l \qquad (13)$$

to solve for E_l. The correct value for X will produce a plot of measured ^{13}C enrichment versus expected ^{13}C enrichment (E_l) with a slope equal to unity.

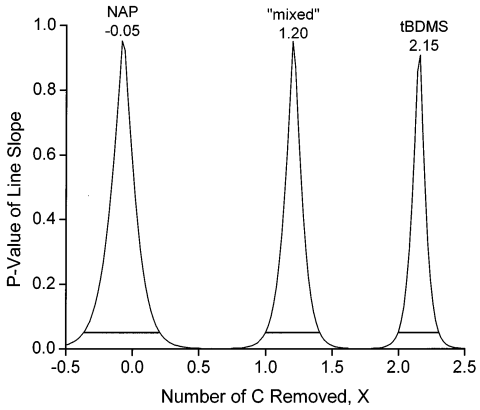

Figure 6. Significance of the slope of the line of the GC/C-IRMS-measured leucine ^{13}C enrichment calibration curves being different from unity as a function of removal of C. The *x*-axis plots the amount of C removed from the derivatized leucine molecule (*X*) by silicon for each derivative measured in Figure 4. The total number of C in each derivative is given in Table 1. The *y*-axis plots the *P* value that the slope of the measured versus expected ^{13}C enrichment line is different from unity. *P* values of >0.05 are considered not significant. Three peaks are shown: one for each derivative type in Figure 4. Each peak top indicates the closest agreement of the measured enrichments to the expected enrichments. The *X* value at that point (shown in the figure at each peak top) indicates the number of C retained by silicon in the molecule. The three derivative curves are labeled on the figure. The line segment at the base of each peak indicates that region of the peak that lies above $P < 0.05$.

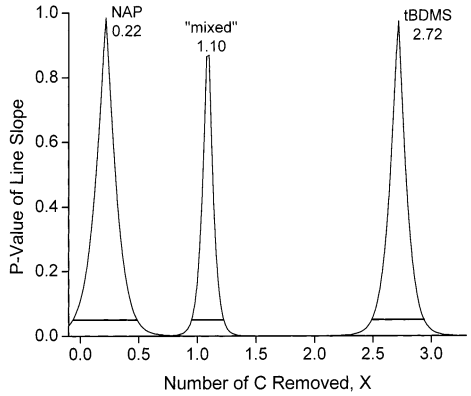

Figure 7. Significance of the slope of the line of the GC/C-IRMS-measured glutamate ^{13}C enrichment calibration curves being different from unity as a function of removal of C. The *x*-axis plots the amount of C removed from the derivatized glutamate molecule (*X*) by silicon for each derivative measured in Figure 5. The total number of C in each derivative is given in Table 1. The *y*-axis plots the *P* value that the slope of the measured versus expected ^{13}C enrichment line is different from unity. *P* values of >0.05 are considered not significant. Three peaks are shown: one for each derivative type in Figure 5. Each peak top indicates the closest agreement of the measured enrichments to the expected enrichments. The *X* value at that point (shown in the figure at each peak top) indicates the number of C retained by silicon in the molecule. The three derivative curves are labeled on the figure. The line segment at the base of each peak indicates that region of the peak that lies above $P < 0.05$.

The problem with simply recalculating the slopes of the measured versus expected ^{13}C enrichment lines in Figures 4 and 5 to produce slopes of unity is that we do not get a measure of uncertainty. We need a determination that places 95% confidence limits on our calculation of carbon retention by silicon. To do this, we have incrementally recalculated the results shown in Figure 4 for the leucine standard curves for a range of *X* values. At each *X* value, we calculated the *P* value of significance of the line being different from unity. In Figure 6, we plot the results of these calculations. The *x*-axis is *X*, the number of C atoms in the molecule that do not appear as CO_2. The *y*-axis is the *P* value of significance that the slope of the measured versus expected ^{13}C enrichment is different from unity. *P* values greater than 0.05 are not significant; i.e., the line at this point is indistinguishable from expected. Thus, each peak in Figure 6 indicates the range of values that *X* could be. A line segment is drawn across the bottom of each peak indicating the $P = 0.05$ point. This line segment denotes the 95% confidence limits for each peak.

We plotted the data for the NAP derivative for leucine as well as the data for the mixed and TBDMS derivatives in Figure 6. Because the NAP-leucine data produced a slope slightly less than unity (Figure 4), the peak shown in Figure 6 has a peak top at a negative *X* value. However, the slope of the NAP-derivative curve in Figure 4 was not significantly different from unity, and the line segment shown in Figure 6 defines the 95% confidence limits that include the value of $X = 0$. Thus, the value of *X* in Figure 6 has a mean value of -0.05 with a confidence range of $-0.36 \leq X \leq 0.20$ for the NAP-leucine ^{13}C curve.

The peak tops for the mixed and TBDMS derivatives of leucine in Figure 6 are $X = 1.20$ and 2.15, respectively. The confidence intervals for these derivative include integer values of $X = 1$ for the mixed derivative and $X = 2$ for the TDBMS derivative, which would be a stoichiometric ratio of one C per Si because there is one silicon in the mixed derivative and two silicons in the TBDMS derivative (Table 1).

In Figure 7, we plot the result of *X* upon the slope of the line being different from expected for the glutamate data shown in Figure 5. Each peak in Figure 7 indicates the range of values of *X* where the measured curve is not different from expected for each derivative. The NAP derivative for glutamate has a peak top at $X = 0.22$, consistent with its slope being slightly (but not significantly greater) than unity (Figure 5). The 95% confidence limits of the NAP derivative ($-0.06 \leq X \leq 0.48$) include the value of $X = 0$.

The peak tops for the mixed and TBDMS derivatives in Figure 7 are 1.10 and 2.72, respectively. The 95% confidence interval for the mixed derivative includes the integer values of $X = 1$, but confidence limit has to be extended beyond 95% to include $X = 3$ for the TDBMS derivative. If we expect a stoichiometric ratio of silicon to carbon, we would expect values of $X = 1$ and 3 for the mixed derivative with one silicon and the TBDMS derivative three silicons, respectively.

The amino acid glutamate was tested in addition to leucine because it contains a second carboxyl group and produces a different set of derivatives containing silicon from leucine. While other variants could also have been used (e.g., lysine with a second amino group), we were limited in terms of the availability of appropriate ^{13}C-labeled standards for testing. The use of glutamate and leucine together is sufficient to define whether the effect we have observed is a function of the location of the silicon in the molecule, i.e., whether the silicon is bonded to nitrogen or to oxygen in the amino acid makes a difference. The mixed derivative provides the case where the silicon is only attached to nitrogen. Both leucine and glutamate ^{13}C curves showed removal of one

carbon from the molecule when one silicon was attached to an amino group. When the silicon was also attached to the carboxyl group of leucine, the number of carbons removed by the silicon rose to two. The number of carbons removed for the TBDMS-glutamate silicon was somewhere between 2.5 and 3, with a peak $X = 2.7$. Therefore, the silicon retention of C appears unaffected by the type of atom to which the TBDMS is attached.

The GC/C-IRMS system we used here is a commercial system available in a similar configuration from several instrument vendors. All use similar technology and all are continuous-flow systems based upon a microcombustion system for organic elemental analysis. The field of organic elemental analysis is a mature discipline originally based upon static combustion of material in sealed tubes. In the last few decades, the static approach has been replaced with commercial continuous-flow instruments.[13,14] In all cases, a high-temperature (900+ °C) combustion chamber is used in conjunction with a metal oxide, typically cupric oxide, or addition of catalyst metals, such as platinum or silver. The oxygen supplied from the cupric oxide is usually sufficient to produce complete oxidation of C in the sample to CO_2. The older literature provides a variety of methods for ensuring accurate measurement of organic elemental composition including nitrogen and sulfur. Other methods are used for compounds where halogens are present.[13,14]

The literature for organic elemental analysis of organosilanes is spottier. For example, in an *Analytical Chemistry* review, a paragraph is given as to how to measure silicon as SiO_2, but no indication of problems is cited.[14] In his 1951 book on the chemistry of silicon, Rochow[15] suggested that static combustion of organosilanes will produce silicon carbide compounds, rather than SiO_2.[15] Angelotti and Hanson warned in a 1974 report that incomplete oxidation of silicon can readily occur in continuous-flow organic elemental analysis systems because of the high stability of silicon carbide even under the high temperatures and oxidative conditions that are used.[16]

What these results do not define is whether the C retained by the silicon is already bonded to the silicon or can come from any C in the molecule. We cannot tell from our results whether the carbon in the ^{13}C-labeled positions participates and is retained by the silicon. We can only define that the slope of the line when plotting the measured ^{13}C enrichment against the expected enrichment is increased by the approximate removal of one C per silicon. However, silicon−carbon bonds are more stable and less prone to oxidation when the attachment to the silicon is from a methyl group, rather than a larger aliphatic groups.[16−18] The silylated derivatives for GC all use methyl groups. Although we have no direct evidence, we suspect on the basis of the literature that the C retained by the silicon in our experiments is one of the two TBDMS methyl group carbons.

The conversion of carbon from the TBDMS into silicon carbide would produce a unit formula of SiC, i.e., one carbon per silicon. Given the tetravalent nature of both carbon and silicon, silicon carbide can form an extended solid as a cubic[19] or rhombic[20] crystal system having an overall empirical formula of SiC (1:1). Because the oxidized TBDMS amino acids are injected into the system in very small amounts (∼2−5 nmol), it is not likely that silicon at the site of oxidation is present in sufficient density to form an extended molecule of SiC units. Instead, the formation of dispersed ionic solid having the same formula unit (SiC) as the extended solid is more probable.

CONCLUSIONS

We expected that the TBDMS derivatives would oxidize to SiO_2, CO_2, and H_2O within the GC/C-IRMS oxidation tube, but our results demonstrate that the silicon of the TBDMS retains carbon, probably in a silicon carbide form. Silicon carbide is a refractory material that once formed will not release carbon at the temperature of the combustion tube. This retention of C skews sample ^{13}C enrichments.

Silicon-based derivatives, such as trimethylsilyl or TBDMS, are important agents to prepare a range of metabolites for measurement by GC because these derivatives are (i) easy to form, (ii) produce a volatile species for most metabolites of interest, and (iii) do not readily degrade the molecule being derivatized.[10,11,21,22] However, our data show that because the silicon in these derivatives retains carbon during their oxidation, a correction factor must be applied to measure of ^{13}C enrichment by GC/C-IRMS when silyl derivatives are used. The correction factor could come from arbitrary application of one C per silicon in the derivative, but results shown here indicate variability in response in making these measurements. Alternatively, a standard curve of known isotopic enrichment could be run simultaneously with the samples, and the slope of the measured ^{13}C enrichment versus expected ^{13}C enrichment could be used to correct the sample ^{13}C measurements. Better yet, silyl derivatives should be avoided when GC/C-IRMS is used to measure carbon-13.

ACKNOWLEDGMENT

This work was supported in part by National Institutes of Health Grants AG-15821, DK-38429 and RR-00109.

Received for review August 16, 2002. Accepted October 23, 2002.

AC026061S

(13) Kirsten, W. J. *Organic Elemental Analysis: Ultramicro, Micro, and Trace Methods*; Academic Press: New York, 1983.
(14) Ma, T. S. *Anal. Chem.* **1990**, *62*, 78R−84R.
(15) Rochow, E. G. *An Introduction to the Chemistry of the Silicones*, 2nd ed.; John Wiley & Sons: New York, 1951.
(16) Smith, R. C.; Angelotti, N. C.; Hanson, C. L. In *Analysis of Silicones*; Smith, A. L., Ed.; John Wiley & Sons: New York, 1974; Chapter 7, pp 113−168.
(17) Rochow, E. G. *An Introduction to the Chemistry of the Silicones*, 2nd ed.; John Wiley & Sons: New York, 1951.
(18) Voronkov, M. G.; Baryshok, V. P.; Klyuchnikov, V. A.; Danilova, T. F.; Pepekin, V. I.; Korchagina, A. N.; Khudobin, Y. I. *J. Organomet. Chem.* **1988**, *345*, 27−38.
(19) Reinicke, R. *Z. Kristallogr.* **1932**, *82*, 394−418.
(20) Rittby, C. M. L. *J. Chem. Phys.* **1992**, *96*, 6768−73.
(21) Schwenk, W. F.; Berg, P. J.; Beaufrère, B.; Miles, J. M.; Haymond, M. W. *Anal. Biochem.* **1984**, *141*, 101−9.
(22) Loy, G. L.; Quick, A. N., Jr.; Teng, C. C.; Hay, W. W., Jr.; Fennessey, P. V. *Anal. Biochem.* **1990**, *185*, 1−9.